

A Multifeature Tensor for Remote-Sensing Target Recognition

Lefei Zhang, Liangpei Zhang, Dacheng Tao, and Xin Huang

Abstract—In remote-sensing image target recognition, the target or background object is usually transformed to a feature vector, such as a spectral feature vector. However, this kind of vector represents only one pixel of a remote-sensing image that considers the spectral information but ignores the spatial relationship of neighboring pixels (i.e., the local texture and structure). In this letter, we propose a new way to represent an image object as a multifeature tensor that encodes both the spectral and textural information (Gabor function) and then apply the support tensor machine for target recognition. A range of experiments demonstrates that the effectiveness of the proposed method can deliver a high and correct recognition rate with a small number of training samples.

Index Terms—Gabor function, multifeature tensor, support tensor machine (STM), target recognition.

I. INTRODUCTION

RECENTLY, with the development of remote-sensing technology, remote-sensing images with very high resolution and hyperspectral channels have been able to provide a large amount of information [1]. We have much more multispectral, high-spatial-resolution, and temporal resolution remote-sensing data than before. Extracting information and knowledge from these images is the main purpose of remote sensing, and identifying or recognizing a given target, particularly artificial targets, is a key aspect in remote-sensing image information processing [2]. For a supervised learning system, we use training samples to construct a classification model with some specific criteria, such as the support vector machine (SVM) [3]–[5], minimax probability machine [6], or Fisher discriminant analysis [7], then distinguish the target and background object from the image.

The traditional training sample is a spectral feature vector; obviously, this vector just denotes one pixel, and it does not consider the structural and textural information from the neigh-

ors. To overcome this, some reports have suggested using spectral as well as spatial information to enhance classification. Puissant et al. [8] proposed to apply a Haralick's second-order statistics to the cooccurrence matrix for textural analysis; Clausi [9] studied the effect of gray quantization on the ability of cooccurrence probability statistics; Kiema [10] examined the gray-level cooccurrence-based texture image fused to TM imagery to expand the object feature base to include both spectral and spatial features; Bau and Healey [11] used a bank of rotation/scale invariant Gabor feature vectors to represent the spectral/spatial properties of a region. These studies verified the enhanced performance of spatial features, but the main shortcoming of these methods is that they only represent the multifeature as a feature vector and neglect spatial and spectral rearrangement of features. Image objects are intrinsically in the form of second-order or higher order tensors, and several different groups have reported experimental results indicating that tensor representation can lead to good classification performance [12]–[14]. However, they only discuss the second-order tensor or matrix, and only few report representing objects using high-order tensors with multifeatures. Therefore, this letter proposes to represent the image object as a multifeature tensor that encodes spectral–textural information and generalizes the vector-based learning machine to a tensor-based learning machine for remote-sensing image target recognition. The experiments are conducted on two data sets: One is a real-world hyperspectral image acquired by a Cambridge Research and Instrumentation (CRI) sensor, and the other is a true-color aerial image in an urban area. The novel contributions of this letter are as follows:

- 1) representing the object in a multifeature tensor;
- 2) Proposing a support tensor machine (STM) for binary classification;
- 3) using the multifeature tensor for remote-sensing image target recognition.

The remainder of this letter is organized as follows. In Section II, the proposed method for multifeature-tensor representation is introduced. Section III discusses the STM in detail. Then, the method of multifeature-tensor target recognition is illustrated in Section IV. Finally, experiments are reported in Section V, followed by the conclusion.

II. MULTIFEATURE-TENSOR REPRESENTATION

A key issue in remote-sensing target recognition is finding an effective representation for target and background objects. In this letter, the multifeature-tensor representation is based on tensor and tensor algebra. A tensor, which can be represented

Manuscript received July 4, 2010; revised August 7, 2010; accepted September 4, 2010. Date of publication October 25, 2010; date of current version February 25, 2011. This work was supported in part by the National Basic Research Program of China (973 Program) under Grant 2011CB707105, by the 863 High Technology Program of the People's Republic of China under Grant 2009AA12Z114, and by the National Natural Science Foundation of China under Grants 40930532 and 40771139.

L. Zhang, L. Zhang, and X. Huang are with the Remote Sensing Group, State Key Laboratory of Information Engineering in Surveying, Mapping, and Remote Sensing, Wuhan University, Wuhan 430079, China (e-mail: zhanglefei.wh@gmail.com; zlp62@public.wh.hb.cn; huang_wuhu@163.com).

D. Tao is with Centre for Quantum Computation and Intelligent Systems, Faculty of Engineering and Information Technology, University of Technology, Sydney, NSW 2007, Australia (e-mail: dacheng.tao@uts.edu.au).

Color versions of one or more of the figures in this paper are available online at <http://ieeexplore.ieee.org>.

Digital Object Identifier 10.1109/LGRS.2010.2077272

as $X \in R^{L_1 \times L_2 \times \dots \times L_M}$, is a multidimensional array with multilinear algebra defined on it. M is the order of the tensor, and the i th dimension of the tensor is of size L_i . An element of X is denoted by X_{l_1, l_2, \dots, l_M} , where $1 \leq l_i \leq L_i$ and $1 \leq i \leq M$ are real numbers. l_i denotes the location of this element in the dimension or mode i . For example, a zero-order tensor $X \in R$ is a scalar, a one-order tensor $X \in R^{L_1}$ is a vector, and a two-order tensor $X \in R^{L_1 \times L_2}$ is a matrix. In [15]–[17], some studies have been performed to use tensors for remote-sensing image multiway filtering and dimensionality reduction.

We have the following definitions of basic tensor algebra [18].

Definition 1: Tensor outer product: The outer product of tensor $X \in R^{L_1 \times L_2 \times \dots \times L_M}$ and tensor $Y \in R^{L'_1 \times L'_2 \times \dots \times L'_M}$ is defined as

$$(X \circ Y)_{l_1, l_2, \dots, l_M, l'_1, l'_2, \dots, l'_M} = X_{l_1, l_2, \dots, l_M} Y_{l'_1, l'_2, \dots, l'_M}. \quad (1)$$

Definition 2: Tensor contraction: The contraction of tensor $X \in R^{L_1 \times L_2 \times \dots \times L_M \times L'_1 \times L'_2 \times \dots \times L'_M}$ and $Y \in R^{L_1 \times L_2 \times \dots \times L_M \times L''_1 \times L''_2 \times \dots \times L''_M}$ is defined as

$$\begin{aligned} & [X \times Y; (1 : M)(1 : M)]_{l_1, l_2, \dots, l_M} \\ &= \sum_{l'_1=1}^{L'_1} \dots \sum_{l'_M=1}^{L'_M} (X)_{l_1, l_2, \dots, l_M, l'_1, l'_2, \dots, l'_M} \\ & \quad \times (Y)_{l_1, l_2, \dots, l_M, l''_1, l''_2, \dots, l''_M}. \end{aligned} \quad (2)$$

The condition for the contraction is that tensors X and Y are of the same size at the specific mode. Contraction reduces the tensor order by $2M$.

Definition 3: Mode- d product (${}_d U$): the mode- d product $X \times {}_d U$ of a tensor $X \in R^{L_1 \times L_2 \times \dots \times L_d \times \dots \times L_M}$ and a matrix $U \in R^{L'_d \times L_d}$ is a tensor of size $L_1 \times L_2 \times \dots \times L_{d-1} \times L'_d \times L_{d+1} \times \dots \times L_M$ defined by

$$(X \times {}_d U)_{l_1, l_2, \dots, l_{d-1}, l'_d, l_{d+1}, \dots, l_M} = \sum_{l_d} \left(X_{l_1, l_2, \dots, l_{d-1}, l_d, l_{d+1}, \dots, l_M} U_{l'_d, l_d} \right). \quad (3)$$

The mode- d product also occurs on tensor $X \in R^{L_1 \times L_2 \times \dots \times L_M}$ and vector $\omega \in R^{L_d}$.

Definition 4: Frobenius norm: The Frobenius norm of a tensor $X \in R^{L_1 \times L_2 \times \dots \times L_M}$ is given by

$$\begin{aligned} \|X\|_{\text{Fro}} &= \sqrt{[X \times X; (1 : M)(1 : M)]} \\ &= \sqrt{\sum_{l_1=1}^{L_1} \dots \sum_{l_M=1}^{L_M} X_{l_1, \dots, l_M}^2}. \end{aligned} \quad (4)$$

Then, we introduce a Gabor function for multifeature-tensor representation. There are two main reasons for introducing the Gabor-based representation for target recognition: It is supposed that simple cells in the visual cortex can be modeled by the Gabor functions, which have good spatial localization, orientation selectivity, and frequency selectivity [13]; second, the features obtained by a Gabor transformation have been found to be effective for texture representation and discrimination and have been successfully applied to object identification, gait recognition, and face recognition [19], [20].

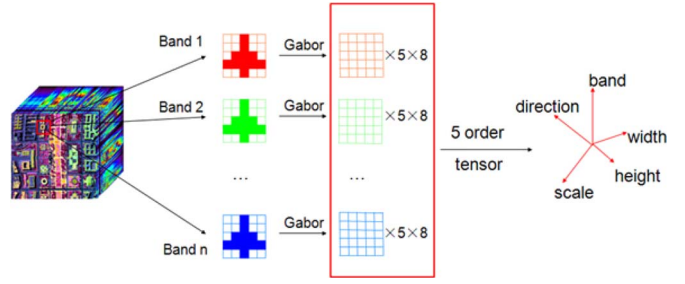


Fig. 1. Representation of a remote-sensing image object as a five-order feature tensor.

The generalized 2-D Gabor function can be defined as

$$\begin{aligned} G_{s,d}(x, y) &= G_{\vec{\kappa}}(\vec{x}) \\ &= \frac{\|\vec{\kappa}\|}{\delta^2} \cdot e^{-\frac{\|\vec{\kappa}\|^2 \cdot \|\vec{x}\|^2}{2\delta^2}} \cdot \left[e^{i \cdot \vec{\kappa} \cdot \vec{x}} - e^{-\frac{\delta^2}{2}} \right] \end{aligned} \quad (5)$$

where $\vec{x} = (x, y)$ is the spatial-domain variable; $\vec{\kappa} = (\pi/2f^s) \cdot e^{i \cdot (\pi d/8)}$ is the frequency vector in which $f = 2$ and s and d are scale and direction parameters of the Gabor function. $s = 0, 1, 2, 3, 4$ and $d = 0, 1, 2, 3, 4, 5, 6, 7$ determine 40 different Gabor functions in five scales and eight directions. The number of oscillations under the Gaussian envelope is determined by $\delta = 2\pi$. The Gabor feature image in a specific scale and direction is the magnitude part of convolving the image with the Gabor function of corresponding parameters s and d .

Remote-sensing images usually have multibands, and each band is a gray image. For the target (or other object in the background) in the image, the object image is defined by the subimage of size width \times height that contains that object. In addition, the multifeature-tensor representation of the object is composed by the Gabor feature images in all bands, scales, and directions. These series of Gabor feature images construct a five-order feature tensor $X \in R^{n \times 5 \times 8 \times w \times h}$, where n gives the spectral band, integers 5 and 8 represent the scale and direction, respectively, and the last two indexes w and h are the spatial location of a pixel in the Gabor feature image. The element of $X_{l_1, l_2, l_3, l_4, l_5}$ denotes the pixel at row l_4 , line l_5 of the Gabor feature image, which is the magnitude part of convolving the object image in band l_1 with a Gabor function of scale l_2 and direction l_3 . Fig. 1 shows the construction of the five-order feature tensor.

III. STM

As we have discussed in Section II, an object is represented as a multifeature tensor but not a conventional feature vector. Considering that a tensor is the generalized version of a vector, we have to generalize the conventional classifiers to the tensor version, which accepts a tensor as a training sample. The STM is generalized from the SVM, which is a classical and effective supervised learning machine. STM aims to find the optimal tensor hyperplane $y(X) = X \prod_{k=1}^M \times_k \vec{\omega}_k + b$, which maximizes the margin between the positive samples and the negative samples. The N training samples with corresponding labels $y_i \in \{+1, -1\}$ are M -order tensors $X_i \in R^{L_1 \times L_2 \times \dots \times L_M}$.

To determine the projection vectors $\vec{\omega}_k (k = 1, 2, \dots, M)$ and bias b of the tensor hyperplane, we can use this optimization [12]

$$\left[\begin{array}{l} \min_{\vec{\omega}_k|_{k=1}, b, \vec{\xi}} \quad \frac{1}{2} \left\| \bigotimes_{k=1}^M \vec{\omega}_k \right\|^2 + c \sum_{i=1}^N \xi_i \\ s.t. \quad y_i \left[X_i \prod_{k=1}^M \times_k \vec{\omega}_k + b \right] \geq 1 - \xi_i, \quad 1 \leq i \leq N \\ \vec{\xi} \geq 0 \end{array} \right] \quad (6)$$

$\vec{\xi} \in R^N$ is a slack variable to deal with the linearly nonseparable problem.

The Lagrangian function for this optimization is

$$\begin{aligned} L(\vec{\omega}_k|_{k=1}, b, \vec{\xi}, \vec{\alpha}, \vec{\beta}) &= \frac{1}{2} \left\| \bigotimes_{k=1}^M \vec{\omega}_k \right\|^2 + c \sum_{i=1}^N \xi_i - \sum_{i=1}^N \beta_i \xi_i \\ &\quad - \sum_{i=1}^N \alpha_i \left[y_i \left(X_i \prod_{k=1}^M \times_k \vec{\omega}_k + b \right) - 1 + \xi_i \right] \end{aligned} \quad (7)$$

with multipliers α_i and β_i , ($i = 1, 2, \dots, N$). Then, we obtain the partial derivative of L

$$\begin{aligned} \partial L / \partial \vec{\omega}_k &= 0 \rightarrow \vec{\omega}_j = \frac{1}{\prod_{k \neq j} \vec{\omega}_k^T \vec{\omega}_k} \cdot \sum_{i=1}^N \alpha_i y_i \left(X_i \prod_{k=1}^M \times_k \vec{\omega}_k \right) \\ \partial L / \partial b &= 0 \rightarrow \vec{\alpha}^T \vec{y} = 0 \\ \partial L / \partial \vec{\xi} &= 0 \rightarrow c - \vec{\alpha} - \vec{\beta} = 0. \end{aligned} \quad (8)$$

The dual problem of (7) is

$$\begin{aligned} \max_{\vec{\alpha}, \vec{\beta}} \min_{\vec{\omega}_k|_{k=1}, b, \vec{\xi}} L(\vec{\omega}_k|_{k=1}, b, \vec{\xi}, \vec{\alpha}, \vec{\beta}) \\ = \min_{\vec{\alpha}} \frac{1}{2} \sum_{i=1}^N \alpha_i y_i \left(X_i \prod_{k=1}^M \times_k \vec{\omega}_k \right) - \sum_{i=1}^N \alpha_i \end{aligned} \quad (9)$$

with the constraint function $\vec{\alpha}^T \vec{y} = 0$. Then, the optimization (9) is a linear program (LP) [21] with the optimization variable $\vec{\alpha} = [\alpha_1, \alpha_2, \dots, \alpha_N]^T$.

Finally, alternating projections are used to find $\vec{\omega}_k (k = 1, 2, \dots, M)$. The details of alternating projection are given in Procedure 1.

Procedure 1: Alternating projection for STM

- 1) Initialize $\vec{\alpha}$ and $\vec{\omega}_k (k = 1, 2, \dots, M)$ randomly;
 - 2) Calculate $\vec{\alpha}$ by LP and substitute $\vec{\alpha}$ from the former to the latter;
 - 3) Set h from 1 to k ;
 - 4) Using the first equation of (8), calculate $\vec{\omega}_h$ through α_i and $\vec{\omega}_k (k \neq h)$, and substitute $\vec{\omega}_h$ from the former to the latter;
 - 5) End of step 3);
 - 6) Carry on with steps 2) to 5) until convergence is reached.
-

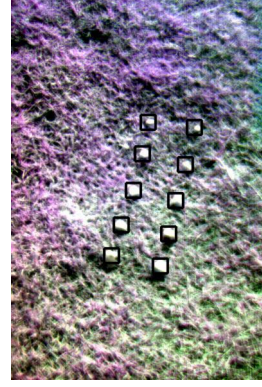


Fig. 2. CRI image of data set 1 with ten targets.

IV. MULTIFEATURE-TENSOR METHOD FOR TARGET RECOGNITION

Target recognition in remotely sensed images could also be considered as a binary classification: to classify the image objects into targets and other objects in the background. The procedure of the multifeature-tensor method for remote-sensing target recognition is as follows:

- 1) represent training samples as five-order multifeature tensors;
- 2) obtain the optimal hyperplane by STM;
- 3) use STM to classify all image objects by shifting the window.

By comparing the feature vector representation and traditional supervised learning methods, there are two advantages for introducing the multifeature-tensor representation and STM into target recognition: The first is that the multifeature of the image object is naturally represented by a multidimensional array, i.e., tensor, so converting this multifeature tensor into a vector discards a great deal of structural information, and the second is that, in STM, the total number of independent parameters of all projection vectors is $N_1 = \sum_{k=1}^M L_k$ because $\vec{\omega}_k \in R^{L_k}$, while in SVM, since the size of the feature vector is $X_i \in R^{(L_1 L_2 \dots L_M)}$, the number of independent parameters in $\vec{\omega}$ is $N_2 = \prod_{k=1}^M L_k$. We can see that $N_1 \ll N_2$; therefore, the tensor representation helps reduce the number of parameters needed to model the data and could reach good classification accuracy using only a small number of training samples.

V. EXPERIMENTS

A. Data Set 1

In this experiment, we used the real-world hyperspectral data acquired by the Nuance CRI hyperspectral sensor. This sensor can acquire imagery with a spectral resolution of 10 nm, covering 650 to 1100 nm in which 16 bands of images with low redundancy were chosen for our experiment. Due to the limitation of the imaging spatial range of the sensor, a small-scale scene (600×400 pixels) with comparatively smaller targets in the acquisition of CRI data is used in this experiment. The imagery of the data set is shown in Fig. 2. There are ten stones in a background of bare soil, grass, and dry grass. As shown in Fig. 2, the size of the image object is 10×10 pixels,

TABLE I
QUANTITATIVE RESULT OF DATA SET 1

STS	Identification Rate		Correct Rate	
	Tensor-based	Vector-based	Tensor-based	Vector-based
5	100%	100%	92.72%	87.30%
10	100%	100%	92.68%	92.25%
15	100%	100%	95.47%	94.75%
20	100%	100%	96.39%	94.91%
25	100%	100%	98.91%	97.47%
30	100%	100%	100%	97.91%

so the size of the extracted five-order multifeature tensor is as large as $16 \times 5 \times 8 \times 10 \times 10$; since the feature vector is represented by vectorizing this tensor, the dimensionality of the vector will be 12 000. We carried out the STM and SVM for target recognition upon the training sets with samples from 5 to 30, and the experimental results are shown in Table I. The results are described using the following two measures.

- 1) Recognition rate: the number of targets that were recognized correctly divided by the total number of targets existing in image.
- 2) Correct rate: the number of targets that were recognized correctly divided by the total number of targets that were recognized. A high value of both recognition rate and correct rate means a good target-recognition performance.

From the correct rates in Table I, it can be seen that both the tensor-based and vector-based method achieved a 100% identification rate in all groups of training sets from 5 to 30; however, the correct rates of SVM are lower than that of STM in all groups of training sets, which indicates that vector representation (SVM) cannot learn a satisfactory model compared with tensor representation (STM) when the size of training samples (STS) is limited. Based on the recognition rates and correct rates of the comparative experiments, the proposed multifeature-tensor representation is demonstrated to be more effective to represent the intrinsic discriminative information of an image object. In addition, it is observed that the STM correct rate is an increasing function of the size of the training set; when STS is more than 30, both the identification rate and correct rate would be steady at 100% since both classifiers are modeled adequately under this circumstance.

B. Data Set 2

In this experiment, the data set is an airborne image of an urban area at Changi airport with background objects of bare soil, lake, grass, roads, and a large number of buildings. The size of the image is 1000×1400 pixels, and the targets to be detected are ten aircrafts, as shown in Fig. 3. Considering the size of the aircraft, we set the size of the object image to 36×36 in this multifeature-tensor-based target-recognition experiment; therefore, the training measurements are $X_i \in R^{3 \times 5 \times 8 \times 36 \times 36}$. Twenty-five measurements are chosen for training samples. The proposed method is compared with two vector-based classification methods: 1) spectral feature vector representation, which only considers spectral features and 20 multifeature vector representation, which reshapes the Gabor-function-based multifeature to a vector; then, the SVM

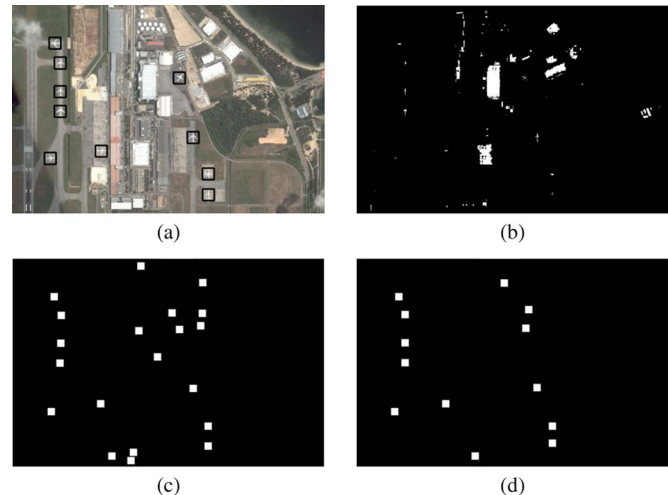


Fig. 3. (a) Original image with targets to be detected. (b) Spectral feature representation. (c) Multifeature vector representation. (d) Multifeature-tensor representation.

TABLE II
QUANTITATIVE RESULTS OF DATA SET 2

Method	Identification Rate	Correct Rate
Spectral feature vector	100%	2.5%
Tensor-based	100%	76.9%
Vector-based	100%	50%

is conducted for classification. The experimental results are shown in Fig. 3 and Table II.

From Fig. 3(a) and (b), it can be seen that both the aircraft and buildings have high digital number (DN) values in RGB, while the traditional spectral feature vector method cannot discriminate those pixels from the aircraft and background since they have similar DN values. The high intraclass and low interclass variances of high-resolution images lead to a reduction in the statistical separability of the different classes in the spectral domain, which causes a high level of wrongly detected pixels in spectral feature space. Therefore, they might be distinguished better through the multifeature rather than only the spectral properties. The proposed multifeature-tensor representation considers the target with multifeature as a high-order tensor and detects all ten aircrafts correctly, with only three locations misclassified as targets. We can also see from Fig. 3(d) that other objects in the background, particularly man-made objects including buildings and roads, are all classified correctly. However, in the multifeature vector-representation method, several places at building corners are misclassified as targets, and the correct rate is only 50%, which demonstrates that the multifeature-tensor representation is a more effective method for target recognition with small training samples. Table II shows the quantitative results with the true condition that we can see in the image. From the table, it is obvious that we have successfully detected all of the targets from the complex background objects with an identification rate of 100% and a correct rate of 76.9% due to the powerful multifeature-tensor representation compared with the vector representation. However, there are still a few false alarms. These are partly because the high DN and similar line features increased the misclassifications of the supervised learning method.

VI. CONCLUSION

In this letter, a new method for representing a remote-sensing image target as a multifeature tensor has been proposed, and the STM is generalized from the SVM for target recognition using the proposed multifeature tensor as training samples. The experiments demonstrate that, for complex backgrounds with similar spectral information, compared with conventional vector-based feature-representation method, the proposed multifeature-tensor representation and STM can achieve a high success rate and correct rate using very few training samples in remote-sensing image target recognition. However, this method could only be used for an invariant scale of target recognition, and a further work will study the multiscale tensor representation.

ACKNOWLEDGMENT

The authors would like to thank the anonymous reviewers for their careful reading and their helpful remarks, which have contributed in improving the quality of this letter.

REFERENCES

- [1] X. Huang and L. Zhang, "An adaptive mean-shift analysis approach for object extraction and classification from urban hyperspectral imagery," *IEEE Trans. Geosci. Remote Sens.*, vol. 46, no. 12, pp. 4173–4185, Dec. 2008.
- [2] L. Zhang, B. Du, and Y. Zhong, "Hybrid detectors based on selective endmembers," *IEEE Trans. Geosci. Remote Sens.*, vol. 48, no. 6, pp. 2633–2646, Jun. 2010.
- [3] C. Burges, "A tutorial on support vector machines for pattern recognition," *Data Mining Knowl. Discov.*, vol. 2, no. 2, pp. 121–167, Feb. 1998.
- [4] V. N. Vapnik, "An overview of statistical learning theory," *IEEE Trans. Neural Netw.*, vol. 10, no. 5, pp. 988–999, Sep. 1999.
- [5] A. Smola, T. Frie, and B. Scholkopf, "Semiparametric support vector and linear programming machines," in *Proc. Conf. Adv. Neural Inf. Process. Syst. II*, 1998, pp. 585–591.
- [6] G. Lanckriet, L. El Ghaoui, C. Bhattacharyya, and M. Jordan, "A robust minimax approach to classification," *J. Mach. Learn. Res.*, vol. 3, pp. 555–582, 2002.
- [7] R. Duda, P. Hart, and D. Stork, *Pattern Classification*, 2nd ed. New York: Wiley, 2001, ch. 5.
- [8] A. Puissant, J. Hirsch, and C. Weber, "The utility of texture analysis to improve per-pixel classification for high to very high spatial resolution imagery," *Int. J. Remote Sens.*, vol. 26, no. 4, pp. 733–745, Feb. 2005.
- [9] D. Clausi, "An analysis of co-occurrence texture statistics as a function of grey level quantization," *Can. J. Remote Sens.*, vol. 28, no. 1, pp. 45–62, Jan. 2002.
- [10] J. Kiema, "Texture analysis and data fusion in the extraction of topographic objects from satellite imagery," *Int. J. Remote Sens.*, vol. 23, no. 4, pp. 767–776, Jan. 2002.
- [11] T. Bau and G. Healey, "Rotation and scale invariant hyperspectral classification using 3D Gabor filters," *Proc. SPIE*, vol. 7334, p. 733 40B-13, 2009.
- [12] D. Tao, X. Li, X. Wu, W. Hu, and S. J. Maybank, "Supervised tensor learning," *Knowl. Inf. Syst.*, vol. 13, no. 1, pp. 1–42, Sep. 2007.
- [13] D. Tao, X. Li, X. Wu, and S. J. Maybank, "General tensor discriminant analysis and Gabor features for gait recognition," *IEEE Trans. Pattern Anal. Mach. Intell.*, vol. 29, no. 10, pp. 1700–1715, Oct. 2007.
- [14] D. Xu and S. Yan, "Semi-supervised bilinear subspace learning," *IEEE Trans. Image Process.*, vol. 18, no. 7, pp. 1671–1676, Jul. 2009.
- [15] N. Renard and S. Bourennane, "Improvement of target detection methods by multiway filtering," *IEEE Trans. Geosci. Remote Sens.*, vol. 46, no. 8, pp. 2407–2417, Aug. 2008.
- [16] N. Renard and S. Bourennane, "Dimensionality reduction based on tensor modeling for classification methods," *IEEE Trans. Geosci. Remote Sens.*, vol. 47, no. 4, pp. 1123–1131, Apr. 2009.
- [17] S. Bourennane, C. Fossati, and A. Cailly, "Improvement of classification for hyperspectral images based on tensor modeling," *IEEE Geosci. Remote Sens. Lett.*, vol. 7, no. 4, pp. 801–805, Oct. 2010.
- [18] L. De Lathauwer, "Signal processing based on multilinear algebra," Ph.D. dissertation, Katholieke Univ. Leuven, Leuven, Belgium, 1997.
- [19] D. Tao, M. Song, X. Li, J. Shen, J. Sun, X. Wu, C. Faloutsos, and S. J. Maybank, "Bayesian tensor approach for 3-D face modelling," *IEEE Trans. Circuits Syst. Video Technol.*, vol. 18, no. 10, pp. 1397–1410, Oct. 2008.
- [20] J. Sun, D. Tao, S. Papadimitriou, P. Yu, and C. Faloutsos, "Incremental tensor analysis: Theory and applications," *ACM Trans. Knowl. Discov. Data*, vol. 2, no. 3, pp. 1–37, Oct. 2008.
- [21] S. Boyd and L. Vandenberghe, *Convex Optimization*. Cambridge, U.K.: Cambridge Univ. Press, 2004.